

## Repair of Earthquake-Damaged RC Columns with FRP Wraps



by Hamid Saadatmanesh, Mohammad R. Ehsani, and Limin Jin

*An investigation was conducted into the flexural behavior of earthquake damaged reinforced concrete columns repaired with prefabricated fiber reinforced plastic (FRP) wraps. Four column specimens were tested to failure under reversed inelastic cyclic loading to a level that can be considered higher than would occur in a severe earthquake. The columns were repaired with prefabricated FRP wraps and retested under simulated earthquake loading. The test specimens were designed to model single-bent, nonductile concrete columns in existing highway bridges constructed before the modern seismic design provisions were in place. FRP composite wraps were used to repair damaged concrete columns in the critically stressed areas near the column footing joint. The physical and mechanical properties of FRP composite wraps are described. Seismic performance of repaired columns in terms of their hysteretic response is evaluated and compared to those of the original and unretrofitted columns. The results indicate that the proposed repair technique is highly effective. Both flexural strength and displacement ductility of repaired columns were higher than those of the original columns.*

**Keywords:** columns (supports); earthquake-resistant structures; fiber reinforced concretes; highway bridges; repairs.

### INTRODUCTION

Research has shown that closely spaced transverse reinforcement in the potential plastic hinge zone of concrete bridge columns substantially increases the compressive strength and effective ultimate compressive strain in the core concrete. The gain in the ultimate compressive strain significantly increases the ductility capacity of concrete columns. Thus, many recent research efforts on seismic retrofitting of concrete columns have been directed to providing additional confinement to the core concrete by means of external reinforcement.

The use of composite materials in construction industry and infrastructure-related applications has greatly increased in recent years (e.g., References 1 and 2). This is primarily due to their high strength, light weight, resistance to corrosion, low cost, versatility, etc. Katsumata et al. reported seismic retrofitting of concrete columns with carbon fiber composite materials.<sup>3</sup> The test results of this new technique showed that winding of carbon fibers around concrete columns greatly increased their earthquake-resistant capacity.

To obtain complete stress-strain curves in compression for concrete reinforced transversely with fiberglass filaments, a total of 33 concrete cylinders confined with fiberglass wires (FGW) were tested by Ahmad and Khaloo.<sup>4</sup> The wires were 80 percent glass fiber by volume and 20 percent polyester resin matrix, and had a tensile strength of 2068 MPa (300 ksi). The test results indicated that the use of FGWs to confine concrete resulted in significant increase in strength and ductility, both of which increased with decreasing FGW spacing around the concrete cylinders.

Saadatmanesh et al.<sup>5</sup> conducted a theoretical study on the behavior of reinforced concrete columns externally confined with high-strength fiber composite straps. Both glass fiber reinforced plastic (GFRP) and carbon fiber reinforced plastic (CFRP) confining straps were investigated in a study to enhance the strength and ductility of existing concrete columns. They concluded that concrete compressive strength and strain would increase substantially when it is wrapped with GFRP or CFRP straps. The modified stress-strain behavior of concrete was used in a parametric study of concrete columns retrofitted with GFRP and CFRP wraps. An examination of the behavior of concrete columns through their ductility and interaction diagrams revealed that the strength and ductility capacity of the columns significantly increased when wrapped with the composite straps.

An experimental program conducted at the University of California at San Diego involved another type of fiber composite materials called Tyfo-s.<sup>6</sup> This type of composite was wrapped like a blanket in layers around a 915-mm-(3-ft)-diameter and 3.66-m-(12-ft)-high test column. The test showed that the fiber wrap provided the desired ductility for the retrofitted concrete columns.

ACI Structural Journal, V. 94, No. 2, March-April 1997.  
Received July 18, 1995, and reviewed under Institute publication policies. Copyright © 1997, American Concrete Institute. All rights reserved, including the making of copies unless permission is obtained from the copyright proprietors. Pertinent discussion will be published in the January-February 1998 ACI Structural Journal if received by Sept. 1, 1997.

ACI member **Hamid Saadatmanesh** is an associate professor in the Department of Civil Engineering and Engineering Mechanics, University of Arizona, Tucson. He is secretary of ACI Committee 440, Fiber Reinforced Plastic Reinforcement. His research interests include application of fiber composites for strengthening and rehabilitation of structures.

**Mohammad R. Ehsani**, F.A.C.I., is a professor in the Department of Civil Engineering and Engineering Mechanics, University of Arizona, and a registered structural engineer in Arizona. He is a member of several ACI committees, including 440, Fiber Reinforced Plastic Reinforcement.

**Limin Jiu** is a structural consulting engineer at One Arup, California. He received his PhD from the Department of Civil Engineering and Engineering Mechanics at the University of Arizona in May, 1995. His research interests include earthquake resistant design and application of FRP composites in structures.

The repair of earthquake-damaged concrete members in high-risk seismic zones is frequently necessary. Very little if any information is available on lateral load resistance and ductility capacity of repaired concrete members. However, such design information is in high demand for the evaluation of the behavior of repaired concrete structures during subsequent earthquakes.

In this paper, an effective technique for repairing earthquake-damaged columns with FRP composite wraps is presented. FRP composite wraps, constructed from high-strength glass fibers weaved to form a fabric-like material of specified width and length, are externally wrapped around the damaged regions of columns in continuous rings, as shown in Fig. 1. The desired confinement to the core concrete at the critical sections is achieved by hoop stresses developed in the composite wrap as a result of the dilation of the core concrete undergoing inelastic deformations. It is noted that the filaments of glass are very strong in tension and could reach an ultimate strength of about 3447 MPa (500 ksi) and a tensile modulus of elasticity of 72.4 GPa (10,500 ksi). The composite straps, which were fabricated in the Structural Engineering Laboratory of the University of Arizona, possessed sufficient flexibility to be easily wrapped around circular as well as rectangular columns. Fig. 2 shows typical composite wraps used in this study.

### RESEARCH SIGNIFICANCE

Considering the large number of concrete columns requiring seismic strengthening and the need for economical techniques for upgrading these structures, the technique described in this paper provides an effective alternative. Furthermore, the utilization of new materials such as fiber composites in this study provides an insight into alternative materials for many different applications in the construction industry.

### FRP COMPOSITE WRAPS FOR SEISMIC REPAIR

To assess the effectiveness of this repair technique, damaged column specimens from another experimental study<sup>7</sup> were repaired with FRP composite wraps. E-glass fibers in the form of a unidirectional fabric were used in the construction of the composite wraps. The fabrication of the composite wraps involved laying flat a long strip of unidirectional E-glass fabric and saturating it with polyester resin matrix. A layer of mylar sheet was then placed on the wet strip, and then the strip was rolled around a mandrel representing the size and shape of the column cross section and placed in an oven to cure. The mylar sheet was provided to prevent bonding

of the composite strip (wrap) to itself while curing. The wet composite wrap was cured at 160 F for 40 min. Fig. 2 shows the finished FRP wraps ready to be used in the column repair. Due to the small thickness, the cured wrap was flexible enough to be wrapped around circular as well as rectangular columns.

The mechanical properties of FRP wrap were determined through tests conducted on specimens designed according to ASTM D3039-76. The data obtained from these tests were used to evaluate various material parameters necessary for the analysis and design of test columns.

Since the FRP wraps are primarily subjected to uniaxial tension in this application, the majority of the fabric fibers in the straps were unidirectionally arranged and impregnated with the resin mixture during the fabrication process. Only a small amount of fibers was used in the transverse direction to hold the fibers together during the manufacturing of the composite wraps. As a result, the uniaxial tension test, in accordance with ASTM D3039-76, was selected for testing of the material properties of the FRP wraps. The tension tests were performed on flat specimens and a uniaxial load was applied through the ends by providing serrated jaw-type end connections.

The stress-strain curves throughout the entire range of loading up to failure were plotted for the specimens with different fiber volume ratios as shown in Fig. 3. In this

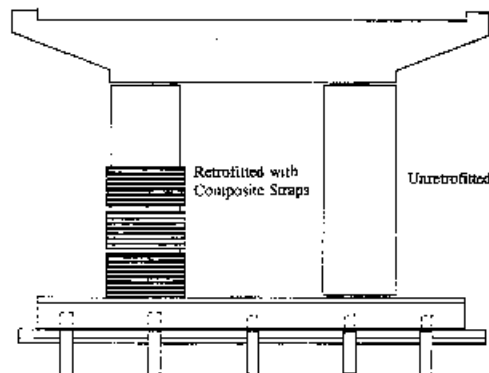


Fig. 1—Retrofitted and unretrofitted concrete columns

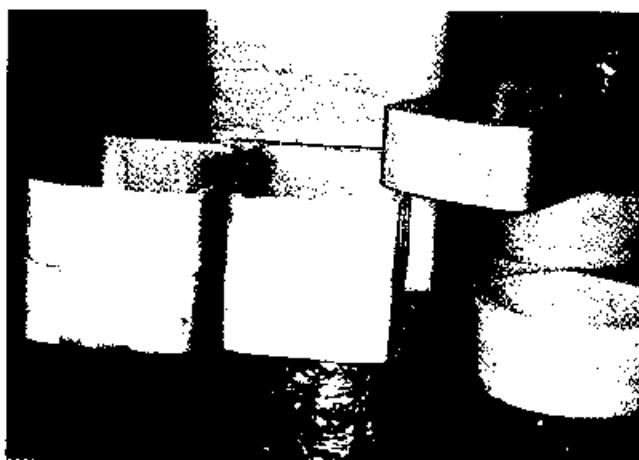


Fig. 2—FRP composite straps for seismic repairs

figure,  $V_f$  defines the ratio of volume of fibers over the total volume of the strap. The data for the stress-strain curves were obtained by averaging the test results from three identical specimens for each of the three fiber volume ratios. The material properties determined from the tests are summarized in Table 1. Composite wraps with  $V_f = 50.2$  percent were used in this study.

Fiber composites are in general durable materials. They are nonconductive and corrosion resistant. For exterior applications, coatings are available to protect the composite wraps from harmful ultraviolet rays. If desired, stucco or other architectural finishes can also be used.

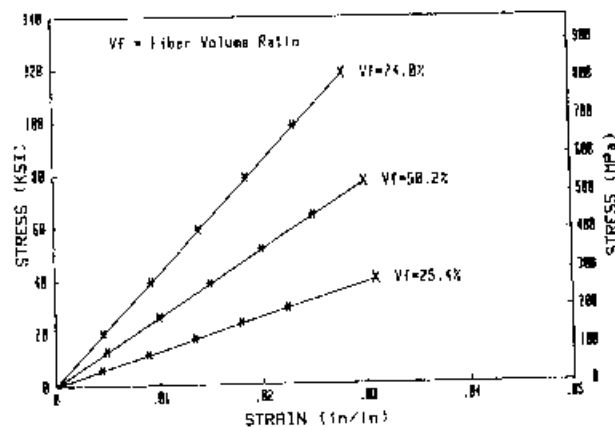


Fig. 3—Typical stress-strain curves for FRP composite wraps

Table 1—Measured properties of FRP composite straps

Fiber volume ratio	$V_f = 25.4$ percent	$V_f = 50.2$ percent	$V_f = 74.0$ percent
Tensile strength, MPa	281	532	814
Tensile modulus, MPa	9074	17,755	29,056
Ultimate strain, mm/mm	0.031	0.030	0.028

Note: 1 MPa = 6.89 ksi.

Table 2—Material properties of column specimens

Column specimen	Concrete strength, MPa	Longitudinal steel		Transverse steel			FRP composite wraps		
		$F_y$ , MPa	$\rho_s$ , percent	$F_y$ , MPa	$\rho_{tr}$ , percent	Spacing, mm	$F_{fr}$ , MPa	Thickness/layer, mm	Total layers
C-1	36.5	358	2.48	301	0.1704	88.9	—	—	—
C-1/R	36.5	358	2.48	301	0.1704	88.9	532	0.8	6
C-2	36.6	358	2.48	301	0.1704	88.9	—	—	—
C-2/R	36.6	358	2.48	301	0.1704	88.9	532	0.8	6
R-1	34.9	359	2.70	301	0.133	114.3	—	—	—
R-1/R	34.9	359	2.70	301	0.133	114.3	532	0.8	8
R-2	33.4	359	5.45	301	0.133	114.3	—	—	—
R-2/R	33.4	359	5.45	301	0.133	114.3	532	0.8	8

Note: 1 ksi = 6.89 MPa; 1 in. = 25.4 mm.

## COLUMN SPECIMENS

Each specimen consisted of a single column bent with a strong footing details, as shown in Fig. 4. The design details simulated the existing seismic deficiencies such as the lack of adequate transverse reinforcement and insufficient starter bars lap length. Four column specimens were used in this study. Columns C-1 and C-2 were circular, while R-1 and R-2 were rectangular. These specimens were tested to failure under simulated earthquake loading (reversed inelastic cyclic loading). They were then repaired with the composite wrap and designated as C-1/R, C-2/R, R-1/R, and R-2/R, "/R" indicating a repaired column. A summary of the material and design properties of these columns is given in Table 2.

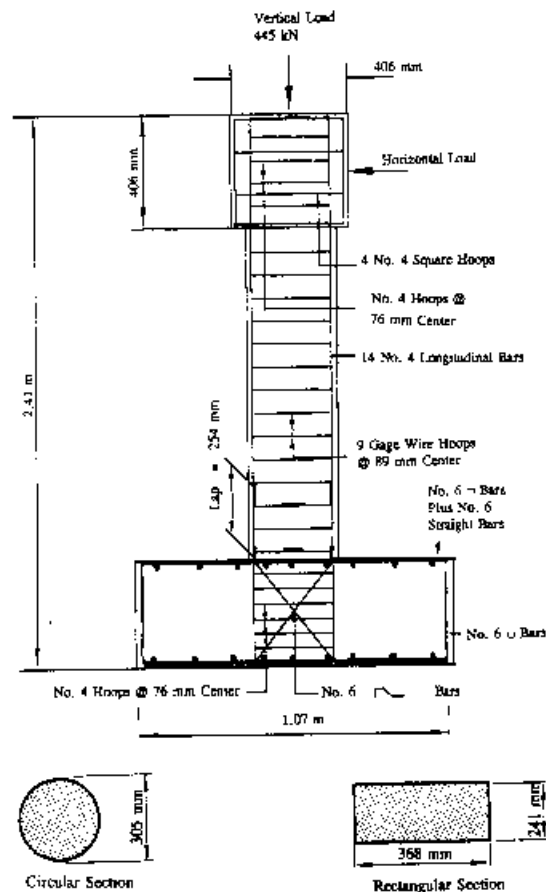


Fig. 4—Design details of test columns

All  
column  
mined  
Struct  
test un  
was 1.  
loading  
x 381  
the fo  
The  
umn c  
reinfor  
footing  
show t  
circula  
spliced  
ment w  
bond f  
nal bar  
had sta  
ameter  
No. 4 b  
for rec  
= 16 m  
reinfor  
Based  
(diamo  
reinfor  
The  
concre  
(nomin  
ified co  
was 21  
= 34.5  
pected  
propor

E  
Each  
erally s  
action  
of the s  
445 kN  
sequen

Fig. 5—

ACI Str

All column specimens were  $1/5$  scale of prototype bridge columns. The dimensions of concrete footings were determined so that the test units fit the hold-down points in the Structural Engineering Laboratory. The overall height of the test units was 2.413 m (7 ft 11 in.). The height of the columns was 1.892 m (6 ft) from the center of pins where the cyclic loading was applied to the top of the footing. A 1067 x 914 x 381 mm (42 x 36 x 15 in.) concrete block was designed as the footing for the specimens, as shown in Fig. 4.

The major design parameters in the specimens were column cross section, longitudinal reinforcement ratio, and reinforcement development details that extended into the footing. The use of different column cross sections attempted to show the effectiveness of the proposed repair technique for circular as well as rectangular bridge columns. Both lap-spliced starter bars and continuous longitudinal reinforcement were used in the design for the columns to examine the bond failure mechanisms in the lapped region and longitudinal bar buckling during the test. Columns C-1 and R-1 each had starter bars with a lap length equal to 20 times the bar diameter, 254 mm (10 in.) for circular columns reinforced with No. 4 bars (diameter = 13 mm [ $1/2$  in.]) and 318 mm (12.5 in.) for rectangular columns reinforced with No. 5 bars (diameter = 16 mm [0.625 in.]). Columns C-2 and R-2 had continuous reinforcement consisting of No. 4 and No. 5 bars, respectively. Based on the selected design scale of  $1/5$ , 9-gage steel wires (diameter = 3.5 mm [0.135 in.]) were used as the transverse reinforcement for the columns.

The materials used in the construction of columns included concrete with  $f'_c = 34.5$  MPa (5000 psi) and Grade 40 steel (nominal yield stress = 276 MPa [40 ksi]). Although the specified concrete compression strength for the prototype columns was 21 MPa (3000 psi), ready-mixed concrete with design  $f'_c = 34.5$  MPa (5000 psi) was used to include the effect of expected overstrength resulting from normal conservative mix proportions and strength gain with concrete aging.

## EXPERIMENTAL PROGRAM AND REPAIR PROCEDURES

Each column (C-1, C-2, R-1, and R-2) was first tested laterally subjected to inelastic earthquake load reversals in a reaction frame, as shown in Fig. 5. Hydraulic rams at the base of the specimens were used to apply a constant axial load of 445 kN (100 kips) to simulate the dead load. A typical loading sequence for one of the specimens (Column C-1) is shown in

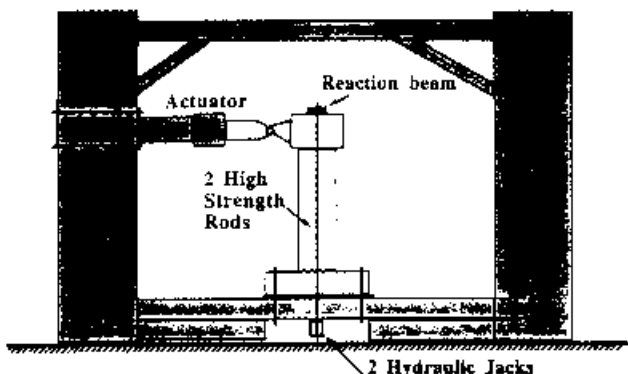


Fig. 5—Test setup

Fig. 6. The loading cycles were divided into two phases: load control and displacement control. Load control phase was used up to yielding of the longitudinal bars; beyond that point, a displacement control loading sequence was used. In Fig. 6,  $u$ , defined as the displacement ductility factor, is the ratio of the applied displacement at the top of the column over the displacement at first yield. At the end of the initial tests to failure, the original specimens (C-1, C-2, R-1, and R-2) experienced severe damage, such as debonding of starter bars, spalling and crushing of concrete in the compression zone, local buckling of longitudinal steel, and the separation of the main bars from the column core concrete, as shown in Fig. 7 through 10. The column specimens to be repaired were pushed back to the original position (i.e., zero lateral displacement) before the repair operation began.

The repair procedures consisted of chipping out loose concrete in the failure zones, filling the gap with fresh concrete, and applying an active retrofit scheme. An active retrofit scheme consists of wrapping the column with slightly oversized FRP straps (3 mm [ $1/8$  in.] away from column face) and filling the gap between the column and the composite wrap with pressurized epoxy. Fig. 11(a) through 11(c) illustrate various steps of the repair operation for a typical damaged column. The first step in repair involved replacing spalled and damaged concrete with quick-setting new concrete and

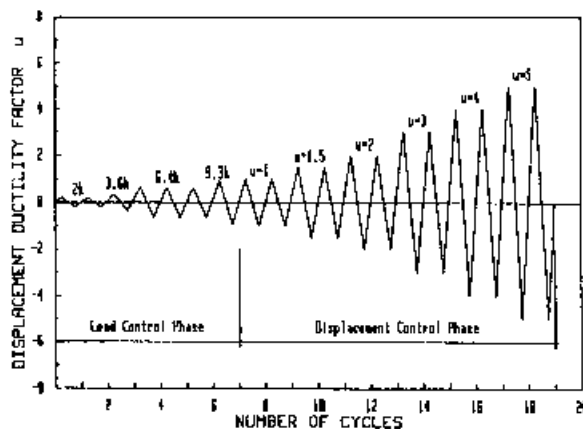


Fig. 6—Loading sequence for Circular Column C-1



Fig. 7—Bond failure of lapped starter bars in Column C-1



Fig. 8—Buckling of continuous longitudinal bars in Column C-2

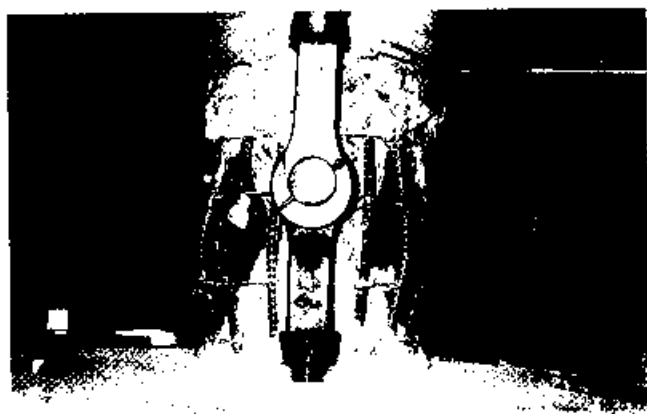


Fig. 9—Column C-2 at conclusion of test



Fig. 10—Separation of main bars from core concrete in Column R-2

finishing the surface to the original shape and dimension [Fig. 11(a)]. The replaced concrete was not vibrated; however, effort was made to fill the cavity as fully as possible. 3 mm ( $1/8$  in.) rubber spacers were bonded to the finished surface of the columns to allow for the gap to be pressurized later; the composite strap was then wrapped on top of the spacers as shown in Fig. 11(b). Based on design requirements, either six or eight plies of the strap were wrapped around circular and rectangular columns, respectively. The number of layers of wraps was selected based on the additional confinement pressure required to bring the column to current design standards. A thin layer of two-component, low-viscosity epoxy was brushed onto the strap while it was being wrapped around the column. Each strap was 151 mm (6 in.) wide and was placed butt-to-butt along the height of the column. The final step of the repair was pressure-injecting epoxy in the gap between the composite wraps and the concrete surface. Hose clamps were provided at the top and bottom of the repair zone to prevent outflowing of the epoxy during pressurization [Fig. 11(c)]. The four repaired column specimens, C-1/R, C-2/R, R-1/R, and R-2/R, were subjected to the same loading sequences as those for the original columns, approximately 1 week after the repair operation was completed.

### TEST RESULTS

During testing of the original specimen, spalling of the concrete cover, opening of the 90 deg hooks of transverse reinforcement, yielding of stirrups, buckling of longitudinal bars, and dropping of the lateral load were marked and recorded. Columns C-1 and R-1 failed as a result of debonding of the longitudinal reinforcing bars in the lapped region. Column C-2 failed by buckling of the continuous longitudinal reinforcing bars. Column R-2, with high longitudinal reinforcement ratio, failed in shear, with longitudinal bars separating from the core concrete, as shown in Fig. 10. Detailed descriptions of the behavior of the four original column specimens are given in References 7 and 8.

In general, all repaired columns performed extremely well under the simulated earthquake loading. Load-versus-displacement results for these columns are presented in Fig. 12 through 15. In these figures,  $\delta_y$  indicates lateral displacement at the top of the column at first yielding of the longitudinal steel reinforcing bars and  $V_R$  is the calculated lateral strength of the column.

Fig. 12(a) shows the hysteresis loops of the original column C-1. As can be seen from this figure, the lateral load dropped significantly after the displacement ductility level of  $u = 1.5$ . In subsequent load cycles, the resistance to lateral load dropped until failure reached as a result of debonding in the lapped region, as was shown in Fig. 7. Fig. 12(b) shows the hysteresis loops of the failed column after it was wrapped with the composite straps in the failure region, that is, in the 635 mm (25 in.) from the top surface of the footing along the height of the column. Clear improvements in the response to cyclic lateral loads can be seen from this figure. At the displacement ductility level of  $u = 3$ , where the original column had failed, no structural degradation was observed in the repaired column. In fact, the response of the repaired column had improved over the original, undamaged column. The remaining columns had similar or even more improved

respo  
repa  
on A  
Tabl  
In  
were  
1.  
displ  
colu  
the f  
conc  
origi  
colu  
as sh  
2.  
ment  
ment  
insuf  
loops  
C-2/R  
teresi  
respe  
infor  
degra  
and I  
tance  
shear  
load-

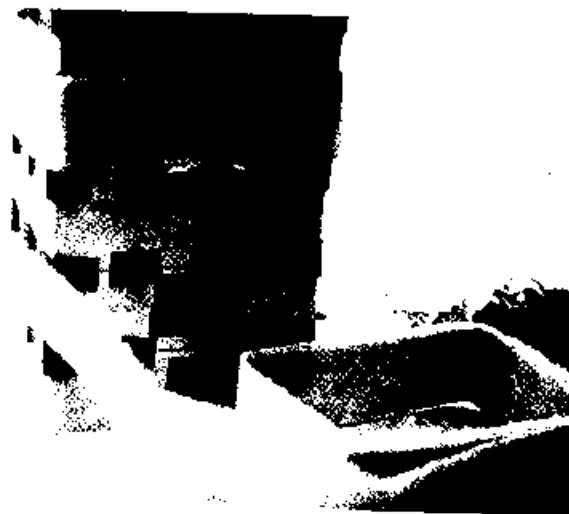
response as compared to the behavior of Column C-1 after repair. The measured and calculated lateral strength (based on ACI 318) of the repaired columns are summarized in Table 3.

In general, typical characteristics of the repaired columns were as follows:

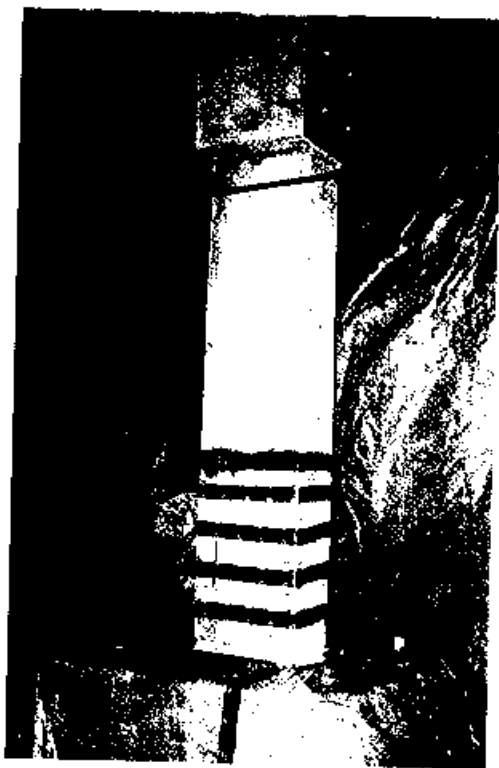
1. The repaired columns exhibited relatively larger lateral displacements at low load levels compared to the original columns. This appeared to be due to pre-existing damage in the form of bond deterioration between reinforcing steel and concrete in the original column, and cracks induced during original testing. However, the lateral strength of repaired columns increased compared to the original control columns, as shown in Table 3.

2. The repaired columns showed a significant improvement in the hysteresis loops of lateral load versus displacement. Both Columns C-1/R and R-1/R, which included insufficient lap lengths at the starter bars, developed stable loops up to a displacement ductility level of  $u = \pm 4$ , and for C-2/R and R-2/R, with continuous longitudinal bars, the hysteresis loops were significantly better even up to  $u = 5$  and 6, respectively. Columns C-2/R and R-2/R with continuous reinforcement bars in the original design showed no structural degradation at the conclusion of the test. Comparing Fig. 15(a) and 15(b) reveals marked improvement in the lateral resistance to cyclic loads of Column R-2, which had failed in shear under the original design. No reduction in the lateral load-carrying capacity was observed for this column even up

to a displacement ductility level of 5, at which point the actuator reached its limit stroke and the test had to be stopped. Repaired columns C-1/R and R-1/R with lapped starter bars in the original design, however, showed small reduction in lateral load-carrying capacity during the last two cycles. The strap in all repaired columns remained intact throughout testing, except Column C-2/R, where some bulging and approximately a 50 mm (2 in.) fracture in the strap in the hoop direction was observed in the last cycle of loading.



(b)



(a)



(c)

Fig. 11—Various steps of repair operation: (a) replace spalled concrete and finish column surface to original shape; (b) wrap continuous FRP composite strap in multitude of layers around failure zone of column; (c) pressurize gap between composite wrap and column with epoxy resin

For each test cycle, the overall stiffness for both positive and negative directions was defined as shown in Fig. 18. The estimated value of the stiffness was determined by dividing the maximum load reached within a cycle by the displacement at the peak of the load cycle in the direction considered. The final stiffness for each cycle was then calculated as the average of the stiffnesses for the positive and negative directions. Tables 4 and 5 summarize average stiffnesses for the circular and rectangular columns.

For comparison, the calculated stiffness for each cycle was normalized with respect to the stiffness of the first cycle and was plotted versus the storey drift ratio as shown in Fig. 19 and 20 for Specimens C-1 and R-1 before and after repair. A close examination of these plots indicates that the column retrofitting has influenced the rate of stiffness degradation. The columns repaired with the composite straps show a slower rate of stiffness degradation than the unretrofitted specimens. Due to concrete crushing and bond failure in longitudinal bars, Columns C-1 and R-1, both designed with lapped starter bars, exhibited a sudden drop in stiffness when the storey drift reached approximately 1.0 percent. They both lost approximately 85 percent of their initial stiffness at the end of the test. The repaired specimens had more than

twice the stiffness of the original columns at the conclusion of the tests.

## CONCLUSIONS

The following conclusions are drawn from the test results of the seismically deficient columns before and after repair:

1. FRP composite wraps are effective in restoring the flexural strength and ductility capacity of earthquake-damaged concrete columns.

2. After repair with FRP wrap, columns with lapped starter bars developed stable hysteresis loops up to the displacement ductility of  $u = \pm 4$ . In columns with continuous reinforcement, the hysteresis loops were stable even up to  $u = 6$  without showing any sign of structural degradation.

3. In all repaired specimens, the rate of stiffness deterioration under large reversed cyclic loading was lower than that of the corresponding original columns. However, the initial stiffness of repaired columns was lower than that of the original columns.

## ACKNOWLEDGMENTS

The research reported in this paper was sponsored by the National Science Foundation under Grants MSS 9022667 and MSS 9257344. The experimental work was conducted in the Structural Laboratory of the Civil

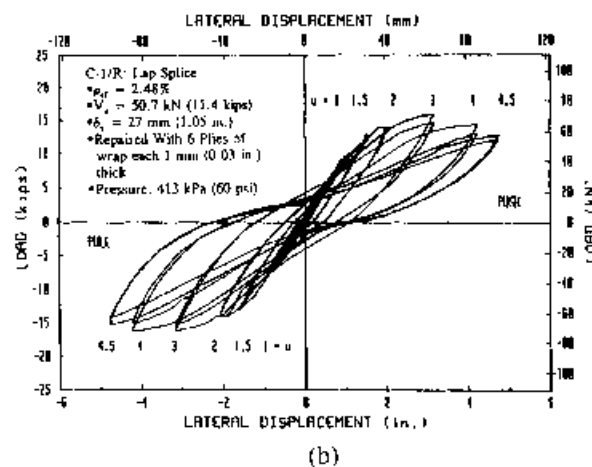
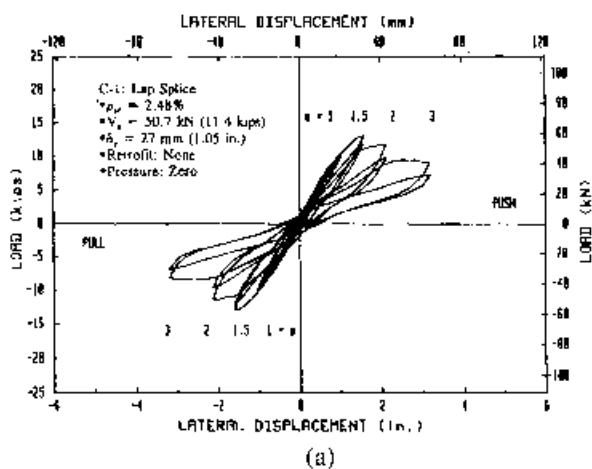


Fig. 12—Load-versus-displacement responses of C-1 before and after repair: (a) load-versus-displacement response of Column C-1; (b) load-versus-displacement response of Column C-1/R

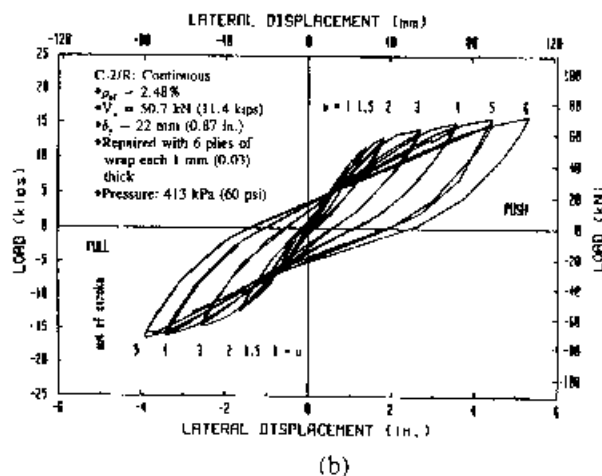
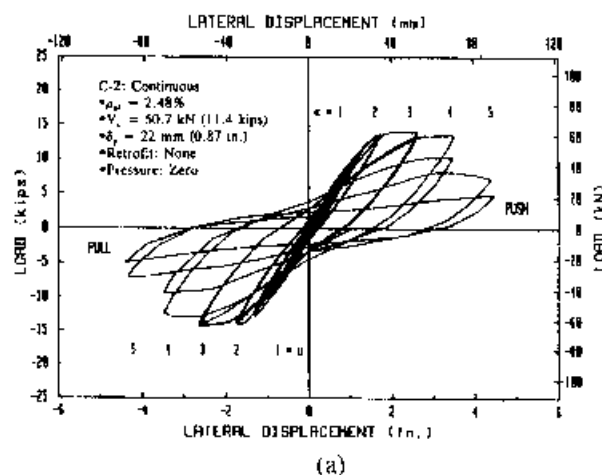


Fig. 13—Load-versus-displacement responses of C-2 before and after repair: (a) load-versus-displacement response of Column C-2; (b) load-versus-displacement response of Column C-2/R

## REFERENCES

1. Chambers, R. E., "Composites Performance in Infrastructure," *Proceedings of the ASCE Material Science Conference*, Atlanta, Georgia, Aug.

**Table 3—Measured and calculated lateral strength of columns**

Specimens	Calculated lateral strength (kN) before repair	Measured maximum load (kN) after repair	Increase in strength
C-1	50.7	58.3	Control
C-1/R	Repaired	72.5	34 percent
C-2	50.7	71.6	Control
C-2/R	Repaired	72.5	1 percent
R-1	89.4	92.1	Control
R-1/R	Repaired	128.5	38 percent
R-2	132.5	161.5	Control
R-2/R	Repaired	211.3	31 percent

1992, pp. 532-545.

2. Tarricone, P., "Plastic Potential," *Civil Engineering*, Aug. 1993, pp. 62-63.

3. Katsumata, H., Kobatake, Y., and Takoda, T., "A Study on Strengthening with Carbon Fiber for Earthquake-Resistant Capacity of Existing Reinforced Concrete Columns," *Proceedings of the 9th Conference on Earthquake Engineering*, V. 7, Tokyo, Japan, Aug. 1988, pp. 517-522.

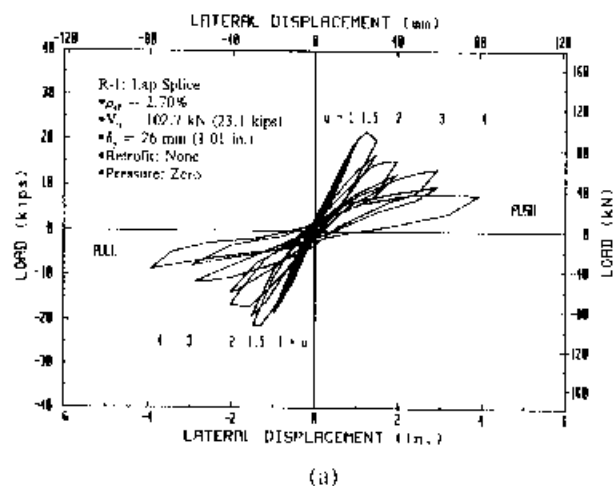
4. Ahmad, S. H., and Khaloo, "Behavior of Concrete Spirally Confined by Fiberglass Filaments," *Magazine of Concrete Research*, V. 43, No. 156, 1991, pp. 143-148.

5. Saadatmanesh, H.; Ehsani, M. R.; and Li, M. W., "Strength and Ductility of Concrete Columns Externally Reinforced with Fiber Composite Straps," *ACI Structural Journal*, V. 91, No. 4, July-Aug. 1994, pp. 434-447.

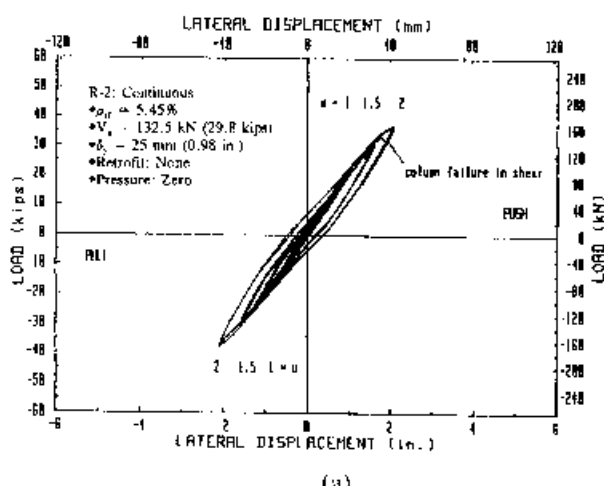
6. Priestly, M. J. N.; Seible, F.; and Fyfe, E., "Column Seismic Retrofit Using Fiberglass/Epoxy Jackets," *Proceedings of Advanced Composite Materials in Bridges and Structures*, Canadian Society for Civil Engineering, 1992, pp. 287-298.

7. Saadatmanesh, H.; Ehsani, M. R.; and Jin, L., "Seismic Retrofitting of Rectangular Concrete Columns Retrofitted with Composite Straps," *Earthquake Engineering Research Institute Journal*, "SPECTRA," V. 13, No. 2, 1977.

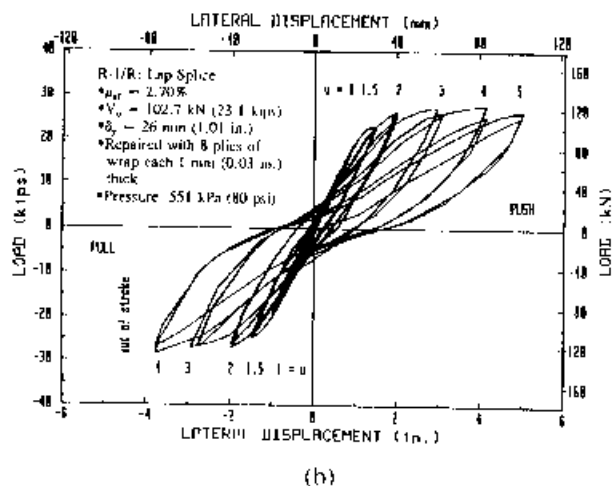
8. Saadatmanesh, H.; Ehsani, M. R.; and Jin, L., "Seismic Strengthening of Circular Bridge Piers with Fiber Composites," *ACI Structural Journal*, V. 93, No. 6, Nov.-Dec. 1996, pp. 639-647.



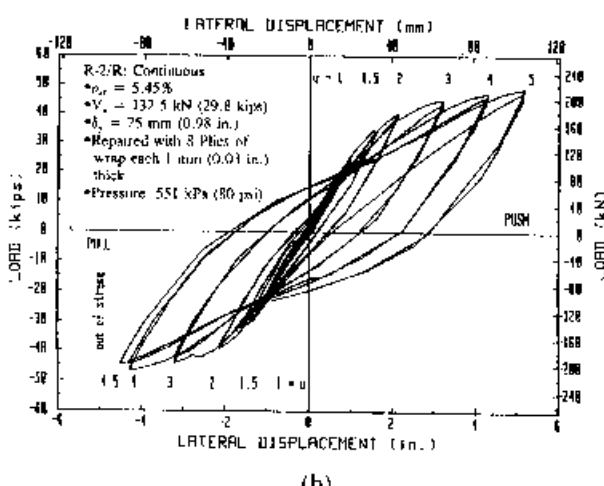
(a)



(a)



(b)



(b)

Fig. 14—Load-versus-displacement responses of R-1 before and after repair: (a) load-versus-displacement response of Column R-1; (b) load-versus-displacement response of Column R-1/R

Fig. 15—Load-versus-displacement responses of R-2 before and after repair: (a) load-versus-displacement response of Column R-2; (b) load-versus-displacement response of Column R-2/R

**Table 4—Stiffness of circular columns at each load cycle**

Cycle	Stiffness at each cycle, kN/mm			
	C-1	C-1/R	C-2	C-2/R
1	2.11	1.87	2.19	1.7
2	2.11	1.87	2.12	1.69
3	2.10	1.78	2.01	1.51
4	2.07	1.7	2.08	1.48
5	2.01	1.58	2.02	1.48
6	1.93	1.44	1.87	1.34
7	1.88	1.44	1.84	1.31
8	1.76	1.17	1.81	1.16
9	1.74	1.16	1.8	1.12
10	1.44	0.89	1.65	0.91
11	1.33	0.83	1.6	0.84
12	0.95	0.63	1.4	0.73
13	0.8	0.58	1.37	0.69
14	0.47	0.53	0.94	0.51
15	0.39	Test stopped	0.91	0.5
16	Column failed		0.65	0.39
17	—	—	0.49	Test stopped
18	—	—	0.28	—
19	—	—	0.19	—
20	—	—	Column failed	—

**Table 5—Stiffness of rectangular columns at each load cycle**

Cycle	Stiffness at each cycle, kN/mm			
	R-1	R-1/R	R-2	R-2/R
1	4.04	3.85	Failed in shear	4.38
2	4.00	3.83	—	4.36
3	3.92	3.81	—	4.35
4	3.77	3.76	—	4.17
5	3.76	3.72	—	4.17
6	3.73	3.7	—	4.06
7	3.56	3.59	—	4.05
8	3.4	3.49	—	3.58
9	3.38	3.46	—	3.54
10	2.44	2.87	—	3.26
11	2.12	2.85	—	3.21
12	1.41	2.39	—	2.43
13	1.16	1.65	—	2.34
14	0.43	1.56	—	1.92
15	0.41	1.27	—	1.85
16	0.37	1.16	—	1.63
17	Column failed	0.93	—	Test stopped
18	—	Test stopped	—	—
19	—	—	—	—
20	—	—	—	—

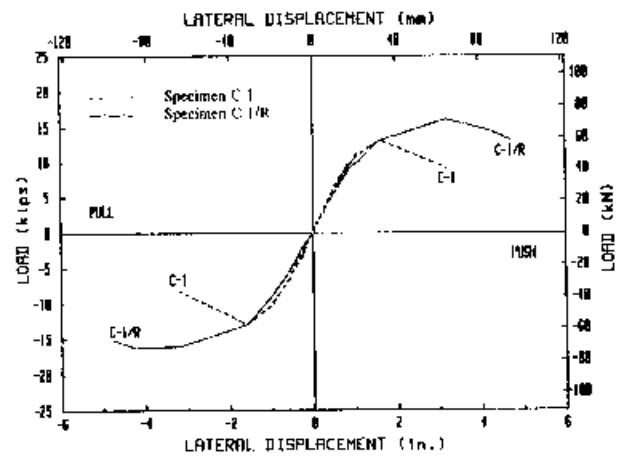


*Fig. 16—Strength envelopes of Column C-1 with starter bars*

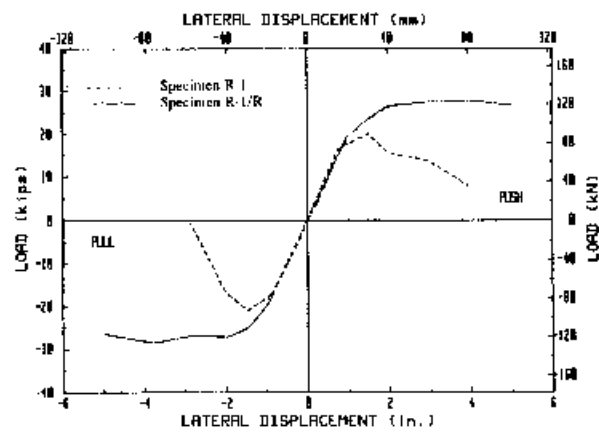


*Fig. 17—Strength envelopes of Column R-1 with starter bars*

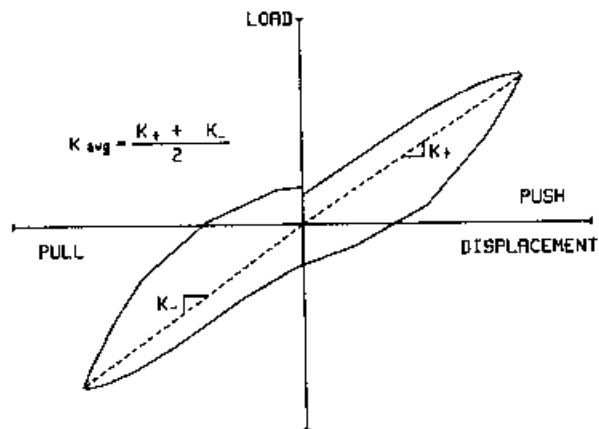


*Fig. 18—Calculation of column stiffness*

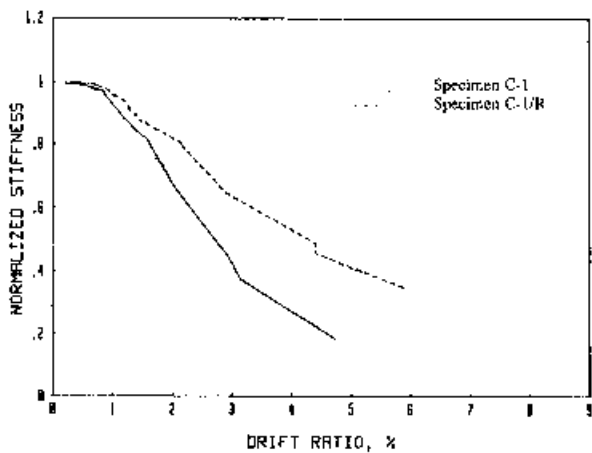


Fig. 19—Normalized stiffness versus storey drift of Column C-1

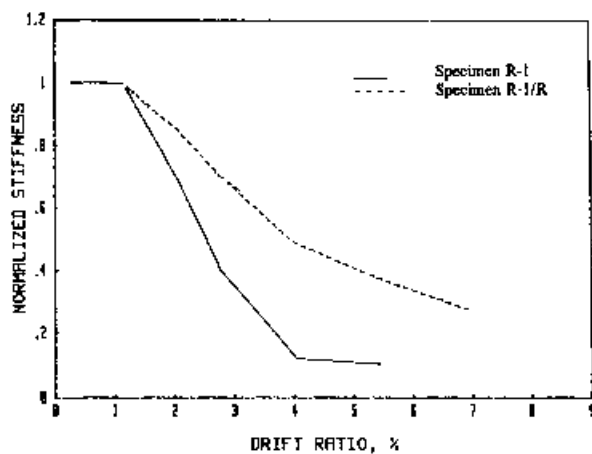


Fig. 20—Normalized stiffness versus storey drift of Column R-1